



Thermodynamic performance analysis of claudé cryogenic system

R. S. Mishra, Devendra Kumar

Department of Mechanical, Production & Industrial and Automobiles Engineering, Delhi Technological University, Delhi, India

Abstract

The present investigation is concerned with Thermal (energy and exergy analyses) of various cryogenic systems up to their sub-component level. A parametric study is conducted to investigate the effects of variation of various system input parameters such as pressure ratio, expander mass flow ratio, compressor output temperature on different performance parameters like COP, work input, liquefaction rate, specific heat and exergy. The numerical computations have been carried out for Claude systems. A study with six different gases for liquefaction like oxygen, argon, methane, fluorine, air and nitrogen respectively. Effect of different input gases also studied carefully and behavior of different gases in different systems is concluded i.e. first law efficiency (COP) and second law efficiency (exergetic efficiency) of Claude system decrease with increase in pressure ratio. For Methane gas COP decreases.

© 2017 ijrei.com. All rights reserved

Keywords: Claude Cryogenic system, Thermodynamic Analysis, Energy-Exergy Analysis, Irreversibility Optimization

1. Introduction

In the year 1920, Claude developed an air liquefaction system and established Air Liquide. The Claude system consists of a compressor, expander, three heat exchangers with a throttle valve and separator. The fluid which has to be liquefied is first fed to the compressor in its gaseous form at atmospheric pressure, it is compressed isothermally in the compressor after that the high pressure gas is partially cooled by passing through the first heat exchanger, at the exit of the first heat exchanger a portion of air is bled and called by expansion in the expander, the remaining portion of air passes through the second and third heat exchangers, the gas from the third heat exchanger is throttled irreversibly at atmospheric pressure. The liquid gas is collected in the separator after throttling. The low temperature gas from the expander is mixed with the gaseous part from the separator, producing an effect of increased mass flow rate at the feed system. In the Claude system, energy is removed from the gas stream by allowing it to do some work in an expansion engine or expander. An expansion valve is still necessary in the Claude system because much liquid cannot be tolerated in the expander in the actual system. The liquid has much compressibility than the gas, therefore, if the liquid were formed in the cylinder of an expansion engine (positive displacement type), high momentary stress would result. Some

rotary turbine expanders (axial-flow type) have developed that can tolerate as much as 15% liquid by weight without damage to the turbine blade. In some Claude systems, the energy output of the expander is used to help compress the gas to be liquefied. In small scale systems, the energy is dissipated in the brake or in an external air blower. This energy is wasted or not it does not affect the liquid yield; however, it increases the compression work requirement when the expander work is not used. A schematic diagram is shown in the below figure. Cryogenic process to liquefy air which is further extended to extract various particular gases like oxygen, nitrogen, iron etc. Always various analyses are done to identify the loop hole of the process and to rectify it to their upper level. Electrocaloric cooling is a transition to new cooling principles is critical and one of the most promising alternatives may be [1]. Various particular parts are taken under study to increase overall performance of cryogenic systems e.g. A good exergetic design of a heat exchanger would allow for an increase in the global efficiency of the process, by defining a thermodynamic cycle in which the exergetic losses would be limited [2] apart from these other parts like expander, mass ratio and input variables are considered to improve cryo-systems.

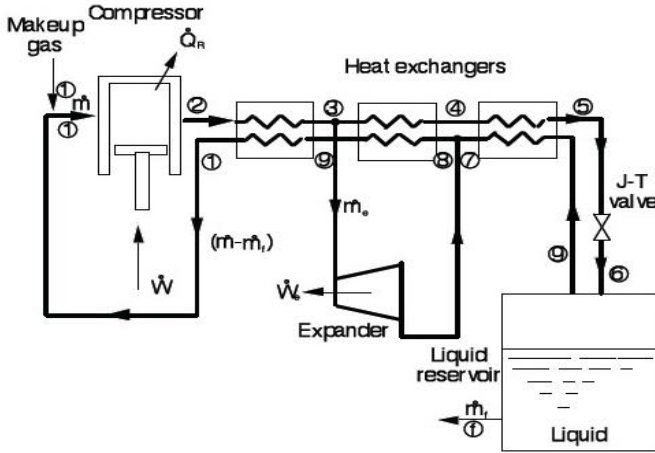


Figure 1(a): Schematic diagram of Claude system

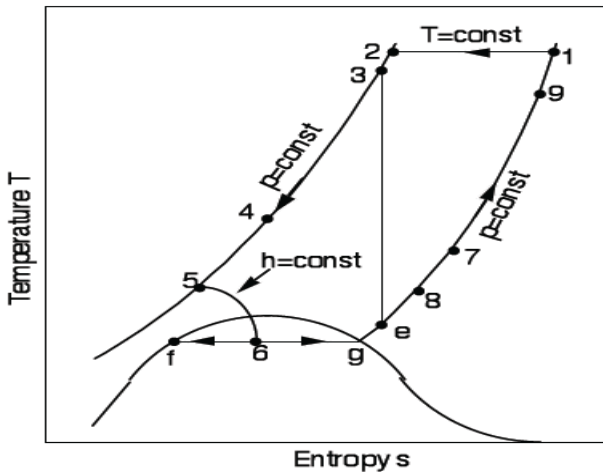


Figure 1(b): T-S diagram of Claude system

In non ideal gas any variable can be defined by two other dependent variables on them:

$$a_{non-ideal\ gas} = f(x(b, c))$$

Following study is carried out to study the behavior of various considered gases in Claude liquefaction system. Exergy analysis help in determining the optimum working parameters of system with different gases.

Table 1: Variable Table

Variable (a)	Gas	Variable (b)	Variable (c)
h_0	R\$	T_0	P_1
h_1	R\$	T_1	P_1
h_2	R\$	T_2	P_2
s_0	R\$	T_0	P_1
s_1	R\$	T_1	P_1
s_2	R\$	h_2	P_2
T_e	R\$	h_e	P_1
h_e	R\$	s_3	P_1
s_e	R\$	h_e	P_1

s_f	R\$	x_f	T_f
T_f	R\$	x_0	P_1
h_f	R\$	x_f	T_f
T_g	R\$	x_1	P_1
s_g	R\$	x_1	T_g
h_g	R\$	x_1	T_g
s_3	R\$	T_3	P_2
h_3	R\$	T_3	P_2
s_4	R\$	T_4	P_2
h_4	R\$	T_4	P_2
s_8	R\$	T_8	P_1
h_8	R\$	T_8	P_1
s_9	R\$	T_9	P_1
h_9	R\$	T_9	P_1
s_{10}	R\$	T_{10}	P_1
h_{10}	R\$	T_{10}	P_1
$cp(hf)_{HX1}$	R\$	T_2	P_2
$cp(cf)_{HX1}$	R\$	T_8	P_1
C_{min}	-	$C_{hot\ HX1}$	$C_{cold\ HX1}$
$cp(hf)_{HX2}$	R\$	T_2	P_2
$cp(cf)_{HX2}$	R\$	T_8	P_1
C_{min}	-	$C_{hot\ HX2}$	$C_{cold\ HX2}$
$cp(hf)_{HX3}$	R\$	T_2	P_2
$cp(cf)_{HX3}$	R\$	$T_g - 1$	P_1
C_{min}	-	$C_{hot\ HX3}$	$C_{cold\ HX3}$
h_7	R\$	T_7	P_1
s_7	R\$	T_7	P_1
X_6	R\$	h_6	P_1
s_6	R\$	h_6	P_1
s_5	R\$	h_5	P_1
h_5	R\$	T_5	P_2

R\$ = ' Gas'

$$m_2 = 1, m = m_2, \frac{m_f}{m} = y, \frac{m_e}{m} = r, r = 0.2, T_0 = 298,$$

$$T_1 = 300, T_2 = T_1, P_1 = 1, P_2 = 40, c_{pfluid} = 1.004 \left[\frac{kJ}{kgK} \right]$$

$$c_{vfluid} = 0.718 \left[\frac{kJ}{kgK} \right]$$

Analysis of Compressor

$$W_c = (m_2 * ((h_2 - h_1)) - T_2 * (s_2 - s_1)),$$

$$Q_c = m_2 * (h_2 - h_1)$$

$$Ed_{comp} = \left(m_2 * T_1 * (s_1 - s_2) - \left(Q_c * \left(\frac{T_0}{T_1} \right) \right) \right)$$

$$COP = \frac{(h_1 - h_f)}{W_c + W_e}$$

$$W_{net} = (W_c + W_e)$$

$$Eta_{2nd\%} = \left(\frac{m_f * ((h_f - h_1) - T_0 * (s_f - s_1))}{W_{net}} \right) * 100$$

Expander

$$W_e = m_e * (h_3 - h_e) - T_0 * (s_3 - s_e)$$

"Heat Exchanger HX1"

$$\text{TypeHX1\$} = \text{' counterflow'}$$

$$m_h = m, m_c = m - m_f$$

$$C_h = m_h * c_{pHX1}, C_c = m_c * c_{pcoldHX1}$$

$$q = C_h * (T_2 - T_3)$$

$$q = C_c * (T_{10} - T_9)$$

$$C_{max} = C_{min} * (T_2 - T_9)$$

$$\text{epsilon} = q/q_{max}$$

$$\text{epsilon} = 0.85$$

$$Ntu_{HX1} =$$

$$HX(\text{TypeHX1\$}, \text{epsilon}, C_{dot_h}, C_{dot_c}, \text{'Ntu'})$$

$$Ntu_{HX1} = (G_{HX1})/C_{min}$$

$$Ex_{inHX1} = m * ((h_2 - h_3) - (T_0 * (s_2 - s_3)))$$

$$Ex_{outHX1} = (m - m_f) * ((h_9 - h_{10}) - (T_0 * (s_9 - s_{10})))$$

$$Ed_{HX1} = ((Ex_{inHX1}) - (Ex_{outHX1}))$$

Heat Exchanger HX2

$$\text{TypeHX2\$} = \text{' counterflow'}$$

$$\text{epsilon}_{HX2} = 0.85$$

$$m_{hHX2} = m - m_e, m_{cHX2} = m - m_f$$

$$C_{hHX2} = m_{hHX2} * c_{p_{hotfluidHX2}}$$

$$C_{cHX2} = m_{cHX2} * c_{p_{coldfluidHX2}}$$

$$q_{HX2} = C_{hHX2} * (T_3 - T_4)$$

$$q_{HX2} = C_{cHX2} * (T_9 - T_8)$$

$$C_{min_HX2} = \min(C_{h_HX2}, C_{c_HX2})$$

$$q_{HX2}^{max} = C_{HX2}^{min} * (T_3 - T_8)$$

$$\text{epsilon}_{HX2} = q_{HX2}/q_{max_HX2} \quad (47) Ntu_{HX2} =$$

$$HX(\text{TypeHX2\$}, \text{epsilon}_{HX2}, C_{dot_{hHX2}}, C_{dot_{cHX2}}, \text{'Ntu'})$$

$$Ntu_{HX2} = (G_{HX2})/C_{min_HX2}$$

$$Ex_{inHX2} = (m - m_e) * ((h_3 - h_4) - (T_0 * (s_3 - s_4)))$$

$$Ex_{outHX2} = (m - m_f) * ((h_8 - h_9) - (T_0 * (s_8 - s_9)))$$

$$Ed_{HX2} = ((Ex_{inHX2}) - (Ex_{outHX2}))$$

Heat Exchanger HX3

$$\text{TypeHX3\$} = \text{' counterflow'}$$

$$T_7 = T_8$$

$$\text{epsilon}_{HX3} = 0.85$$

$$m_{hHX3} = m - m_e, m_{cHX3} = m - m_f$$

$$C_{hHX3} = m_{hHX3} * c_{p_{hotfluidHX3}}$$

$$C_{cHX3} = m_{cHX3} * c_{p_{coldfluidHX3}}$$

$$q_{HX3} = C_{hHX3} * (T_4 - T_5)$$

$$q_{HX3} = C_{cHX3} * (T_7 - T_g)$$

$$q_{max_HX3} = C_{min_HX3} * (T_4 - T_g)$$

$$\text{epsilon}_{HX3} = q_{HX3}/q_{max_HX3}$$

$$Ntu_{HX3} = HX(\text{TypeHX3\$}, \text{epsilon}_{HX3}, C_{hHX3}, C_{cHX3}, \text{'Ntu'})$$

$$Ntu_{HX3} = (G_{HX3})/C_{min_HX3}$$

$$Ex_{inHX3} = (m - m_e) * ((h_4 - h_5) - (T_0 * (s_4 - s_5)))$$

$$Ex_{outHX3} = (m - m_f) * ((h_g - h_7) - (T_0 * (s_g - s_7)))$$

$$Ed_{HX3} = ((Ex_{inHX3}) - (Ex_{outHX3}))$$

Analysis of Valve

$$h_5 = h_6$$

$$Ex_{inval} = (h_5 - h_0) - T_0 * (s_5 - s_0)$$

$$Ex_{outval} = (h_6 - h_0) - T_0 * (s_6 - s_0)$$

$$Ed_{val} = Ex_{inval} - Ex_{outval}$$

Analysis of separator

$$(m - m_e) * h_6 = ((m_f * h_f) + (m_g * h_g))$$

$$m_g = (m - m_e - m_f)$$

$$Ed_{sep} = \left(T_0 * \left(\frac{(m_g * s_g - (m_g + m_f) * s_6) +}{\left(\frac{m_g * h_g - m_f * h_f}{T_0} \right)} \right) \right)$$

$$Ed_{comp\%} = \left(\frac{Ed_{comp}}{Ed_{Claude}} \right) * 100$$

$$Ed_{HX1\%} = \left(\frac{Ed_{HX1}}{Ed_{Claude}} \right) * 100$$

$$Ed_{HX3\%} = \left(\frac{Ed_{HX3}}{Ed_{Claude}} \right) * 100$$

$$Ed_{HX2\%} = \left(\frac{Ed_{HX2}}{Ed_{Claude}} \right) * 100$$

$$Ed_{val\%} = \left(\frac{Ed_{val}}{Ed_{Claude}} \right) * 100$$

$$Ed_{sep\%} = \left(\frac{Ed_{sep}}{Ed_{Claude}} \right) * 100$$

$$Ed_{Claude} = Ed_{comp} + Ed_{HX1} + Ed_{HX2} + Ed_{HX3} + Ed_{val} + Ed_{sep}$$

2. Result and Discussion

Fig.2 show the COP and second law efficiency variation with different pressure ratio from analysis, it is noticed that in Claude liquefaction system COP and second law efficiency decrease with increase in pressure ratio. Methane gas COP decreases from 1.35 to 0.95 for the PR range of 40- 220. While other gases like fluorine, oxygen, air, nitrogen and argon COP decreases from 1.15 to 0.75. For all gases 40 bar PR is optimum pressure point. Second law efficiency of system is highest for fluorine gas i.e. 85% followed by nitrogen, air oxygen respectively which has 80-83% second law efficiency. Methane gas show least second law efficiency 67% which continuously decreases from 67% to 45 % for PR range 40 - 220. Liquefaction rate of different gases at different pressure ratio is shown in fig.3. Gases such as argon, oxygen and methane show sharp decrease in liquefaction rate with increase in PR while gases fluorine, nitrogen and air show slight decrease as compared to above gases with increase in PR .The

liquefaction decrement rate of air is lowest i.e. 45% to 42.5% for entire PR range in among all six gases while argon show highest liquefaction rate of 48% which decreases with increase in PR from 48% to 42.5%. Again 40 PR is the ideal pressure for highest liquefaction rate for all gases. Fig.4 show variation in work requirement for gases at different pressure ratio of Claude system. All gases work requirement increases with increase in pressure ratio of system. Methane gas show highest work requirement 725 kJ/kg to 950 kJ/kg for PR range while Argon show lowest work requirement 275 kJ/kg which increases up to 350 kJ/kg on highest PR 220 in gases. Specific heat of gas is very important factor while energy is transferred between cold and hot fluid. Specific heat of gas is very much influenced by the temperature change during heat exchange in heat exchanger. Fig. 5 show change in specific heat of gases during first heat exchanger with variation in PR. It notice that specific heat for all gases increases during heat exchange with increases in PR of compressor. Methane gas show large change in specific heat 2.4 kJ/kg-K to 3.6 kJ/kg-K compare to other gases with increase in PR 40 to 220. Other gases such as nitrogen, air, and oxygen of first heat exchanger (HX1) show very slight change in specific heat 1.1 kJ/kg-K to 1.3 kJ/kg-K. Fluorine show lowest specific heat 0.8 kJ/kg-K at 40 PR. Change in NTU of first heat exchanger for considered gases with variation in PR as shown in fig.6. At 40 PR, nitrogen and air show equal value of NTU 2.75 but as the pressure ratio increases nitrogen NTU value vary from 2.75 to 2.62 whereas air in same PR range vary from 2.75 to 2.51. Methane gas show lowest value of NTU 2.6 to 2.37 at PR range (40-220). Other gases NTU value decrease with increase in pressure ratio. As the temperature decreases the trend of decrease in NTU for gases also get change. NTU variation with PR in second heat exchanger shown in fig.7. The highest NTU value for air and nitrogen are 5.6 and 5.5 at 80 and 100 PR respectively. The trend of NTU for air and nitrogen with PR show that NTU value first increases up to said PR then they start decreasing again. Gases like oxygen, fluorine argon and methane show decreasing trend with increasing PR. Methane has lowest NTU value which varies from 4.6 to 3.4 for PR range. In third heat exchanger of Claude system the NTU variation with respect to pressure ratio is shown in fig.8. In this Methane gas show highest value of NTU among all gases and it varies from 3.2 to 4.1. From analysis, it is noticed that after 180 PR the change in NTU of methane get constant and show very less variation. All other gases NTU varies from 2.2 to 3 in which argon gas shows least NTU value. Fig.9 shows variation in exergy destruction rate in compressor with increasing pressure ratio. The highest destruction rate is notice for methane gas which ranges from 600 kJ/kg to 1150 kJ/kg for PR range while other gases also show increase in exergy destruction rate with increase in PR. Argon and Fluorine show almost same trend of exergy destruction ranging from 250 kJ/kg to 325 kJ/kg. Exergy destruction in first, second and third heat exchanger is shown in figs [10-12]. In first and second heat exchanger, there is decrease in exergy destruction with increase in PR while in third heat exchanger this variation is reverse, in the low temperature heat exchanger exergy destruction rate increases

with increases in PR. In first heat exchanger gas nitrogen and air show sharp variation in exergy destruction rate up to 80 PR but after this PR the slope of decrement of two gases reduces. Fluorine gas exergy destruction variation over PR is very less as compared to other gases, it vary from 1.8 to 1.6 over entire PR range. Argon show least exergy destruction rate among all six gases. In third heat exchanger the rate of exergy destruction of gases air and nitrogen show unusual behavior, in both gas there is slight dip in exergy destruction rate up to 80 PR then it rise up again up to 160 PR and then become almost constant up to 220 PR. The range of variation in exergy destruction in both gas are 119 to 121 which almost constant. Fig.13 show variation in exergy rate in valve with pressure ratio. The slope of increasing exergy destruction rate for methane and nitrogen is high as compared to other gases. Nitrogen gas destruction rate varies from 30 kJ/kg to 140 kJ/kg between PR of (40-220). In valve, air has least exergy destruction rate and almost constant for considered PR range. Fig.14 show exergy destruction trend for gases with pressure ratio. Oxygen, argon, air, nitrogen exergy destruction range is 675 kJ/kg to 600 kJ/kg, 500 kJ/kg to 450 kJ/kg and 350 kJ/kg to 325 kJ/kg respectively. Outlet temperature of expander also get affected by the PR. Fig.15 show variation in outlet temperature of expander with increasing PR with all six gases. Gases outlet temperature decrease in the range of 65-80 PR from 100 K to 88 K (fluorine), 95K -92 K (oxygen), 94K - 83 K (air) and 95K-76 K (nitrogen) respectively. Argon and Nitrogen show almost constant value of outlet temperature that 87 K and 113 K respectively on entire PR range. Fig.16 show the variation in COP and second law efficiency keeping constant optimum PR 40 with variation in expander mass flow ratio or ratio of compressor flow through expander (r). For all gases except methane second law efficiency decreases from 80 % to 40 % when flow ratio through expander increases from 0.5 to 0.8. In methane gas case the system show lowest efficiency range 70 % to 15% over expander flow ratio range. Moreover, COP of system first decreases marginally up to 0.6 PR then it start increasing with increase in flow ratio of expander. The highest COP is exhibit by methane 1.25 followed by other gases. Argon gas show least COP 1 and it is almost entire flow ratio range. Fig.17 show effect on liquefaction rate when there is increase in flow ratio of expander. From graph it is concluded that the liquefaction rate drop from 0.45 kg/s to 0.2 kg/s an average for all gases over increasing flow ratio. Net Work done also affected by expander flow ratio. Fig.18 show methane require 750 kW energy when the expander flow ratio is 0.5 and it almost same up to 0.8. Other gases follow the same trend of decrement over expander flow ratio range from 0.5-0.8. Compressor outlet temperature effect the performance of system. In fig.19, the variation in COP and second law efficiency of system is measured with the increase in compressor outlet temperature of all considered gas as a working fluid. Highest COP of system show at 280 K for all six gases which start decreasing gradually over increase in compressor temperature. The argon gas show lowest COP 1.02 and methane show highest. Same decreasing trend is followed by second law efficiency also and have highest second law

efficiency of methane 90 % to 75% over compressor temperature range while argon show lowest second law efficiency among all gases which range from 55% to 15% over increasing temperature of compressor. Rest of four gases show same decreasing trend for COP and second law efficiency. Fig.20 shows the effect of compressor temperature variation over outlet temperature of expander. In this graph study, it analyses that the for methane gas the variation in outlet temperature (110K) is constant up to 300 K then it start increasing with increase in temperature of compressor. All other gases except argon show increasing trend in outlet temperature with increase in compressor temperature. Argon has the least outlet temperature and remain constant over the compressor temperature range of 280 K to 420K. After 420 K there is small increase in outlet temperature of expander. Fig. 21-23 show variation in specific heat of first, second and third heat exchanger with respect to outlet temperature of compressor. In all three graph same trend of variation in specific heat of gases is notice. The methane gas show highest specific heat ranging from 2.5 kJ/kg-K to 2.9 kJ/kg-K for compressor temperature range 280 K -460 K, while other gases show average specific heat of nitrogen, air, oxygen, fluorine and argon 1.1 kJ/kg-K, 1.12 kJ/kg-K, 1 kJ/kg-K, 0.9 kJ/kg-K and 0.6 kJ/kg-K respectively at 280 K. The variation in gases except methane is not notice much and almost seem constant over increasing outlet temperature of compressor. Fig.24 show effect of compressor outlet temperature on liquefaction rate of gases .it observed that argon have highest liquefaction rate 0.474 kg/s and air is least 0.455 kg/s at 280 K. All gases have same liquefaction rate 0.4 kg/s at temperature 280K. All gases liquefaction rate is decreasing with increase in compressor outlet temperature. Variation in work requirement of system with increases in outlet temperature of compressor is shown in fig.25 .The methane gas show highest requirement of work 700 kW at 280 K and argon required least 250 kW at 280K .The trend of gases work requirement is progressing with increase in compressor temperature. .Exergy destruction rate in compressor is also showing same trend of increasing in nature for all gases shown fig.26.The methane range of exergy destruction is 600 kJ/kg -900kJ/kg whereas other gases such as nitrogen, air, oxygen, fluorine and argon range from 320 kJ/kg-500kJ/g, 310kJ/kg- 480 kJ/kg, 290 kJ/kg - 440kJ/kg, 230 kJ/kg-370kJ/kg and 210kJ/kg - 350 kJ/kg respectively. The exergy destruction rate in first heat exchanger is very low at low temperature. Most of the gases first show decreases in exergy destruction up to 320 K and then start increasing at very fast rate if compressor temperature is further increased. Methane gas show highest destruction rate ranging from 8 kJ/kg to 42 kJ/kg. The trend of exergy destruction is shown in fig.27. In second heat exchanger the variation in exergy destruction rate of methane and fluorine gas is first increases up to 300 K then start decreasing on increasing compressor temperature. Gases such as oxygen, air and argon are not much affected up to 340 K but beyond this compressor temperature exergy destruction rate start decreasing.

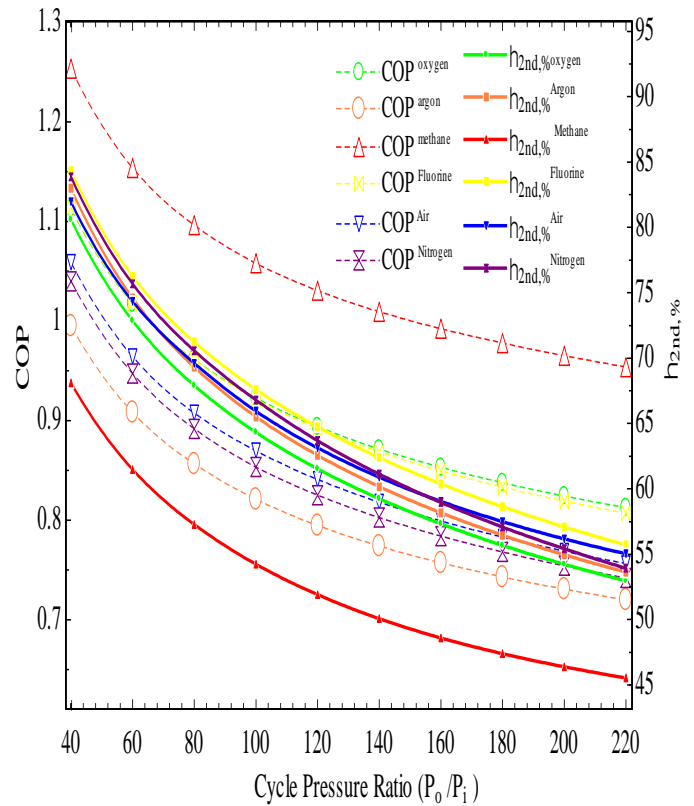


Figure 2: Variations in COP and second law efficiency with respect to cycle pressure ratio

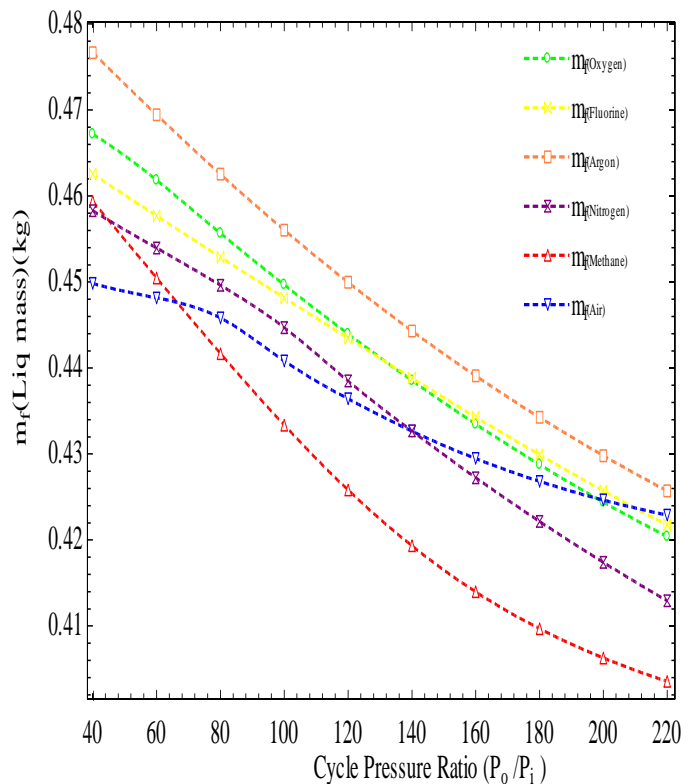


Figure 3: variations in the mass liquefaction rate with respect to cycle pressure ratio

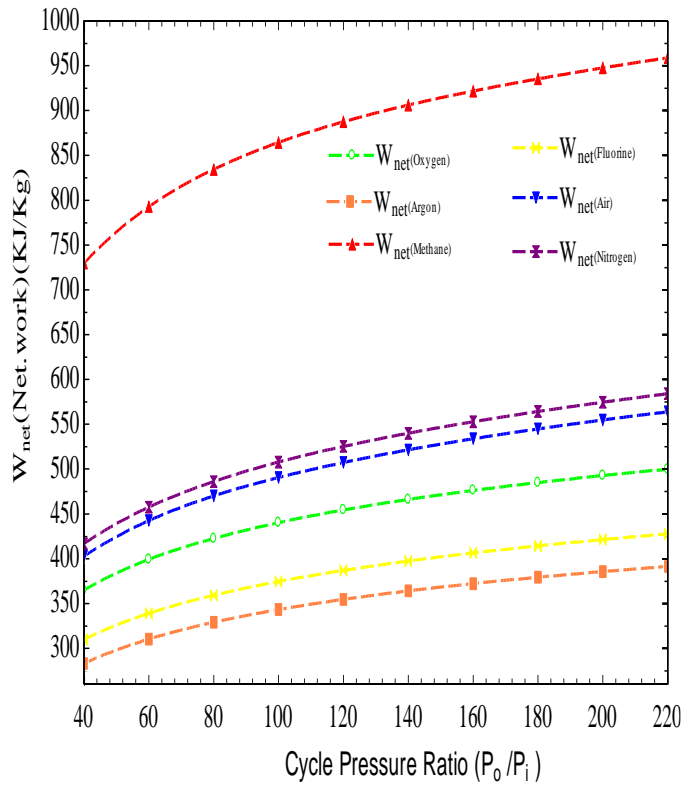


Figure 4: Variations in net work done with respect to cycle pressure ratio

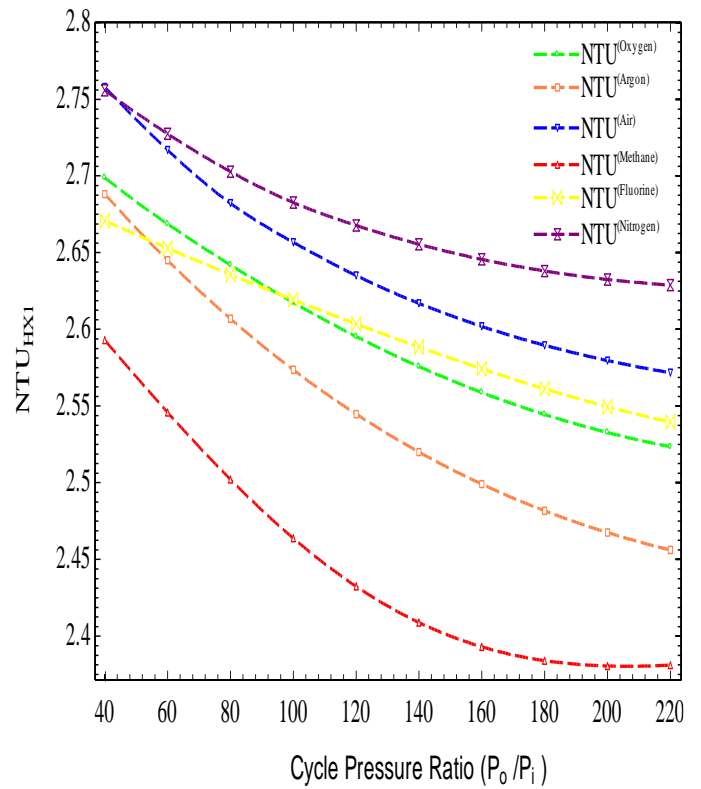


Figure 6: Variations in NTU in HX1 with respect to cycle pressure ratio

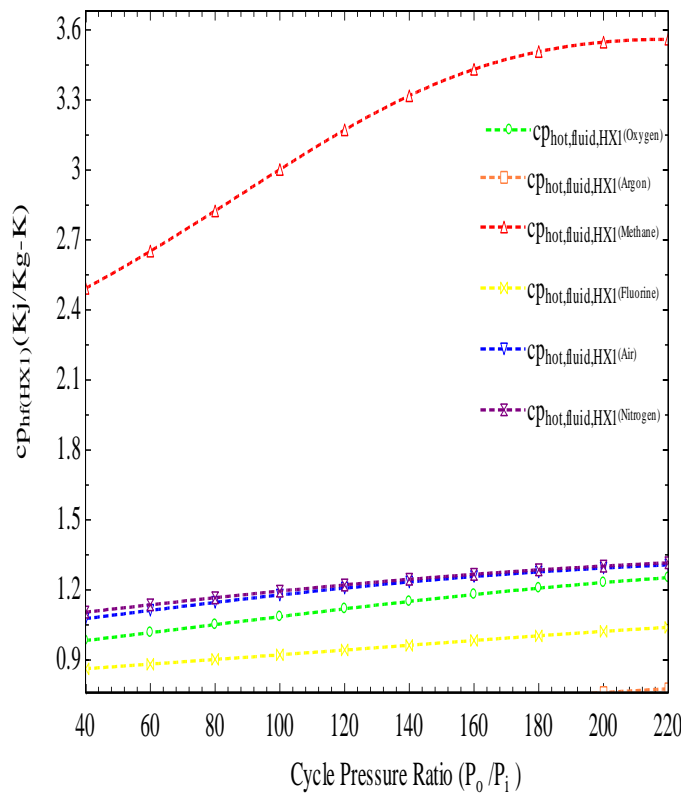


Figure 5: Variations in specific heat of hot fluid in HX1 with cycle pressure ratio

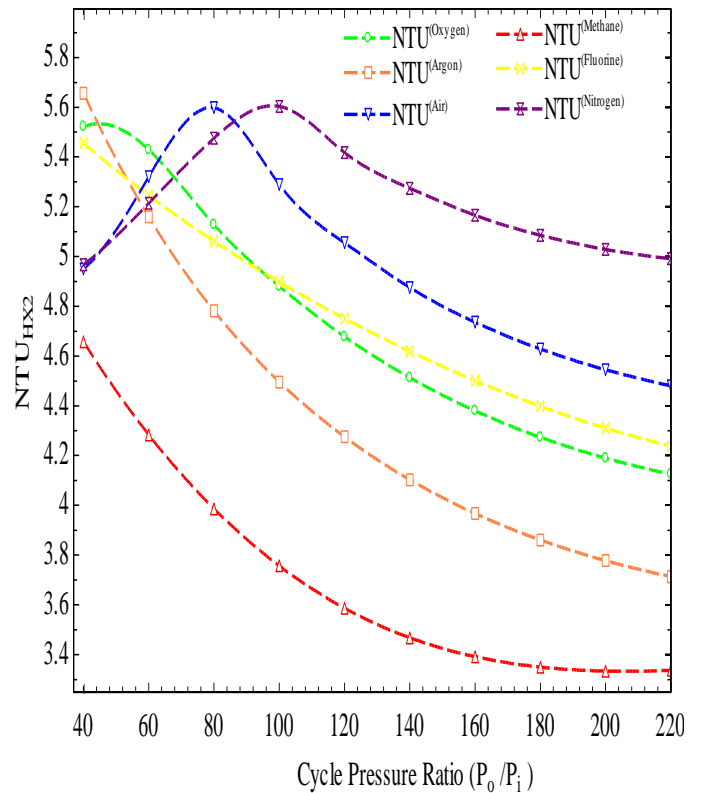


Figure 7: Variations in NTU in HX2 with cycle pressure ratio

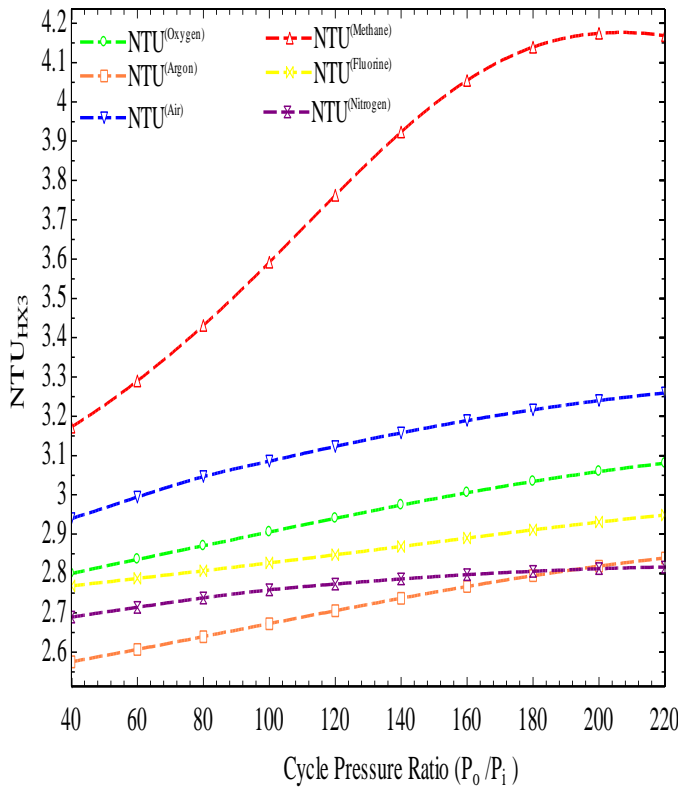


Figure 8: Variations in NTU in HX3 with the cycle pressure

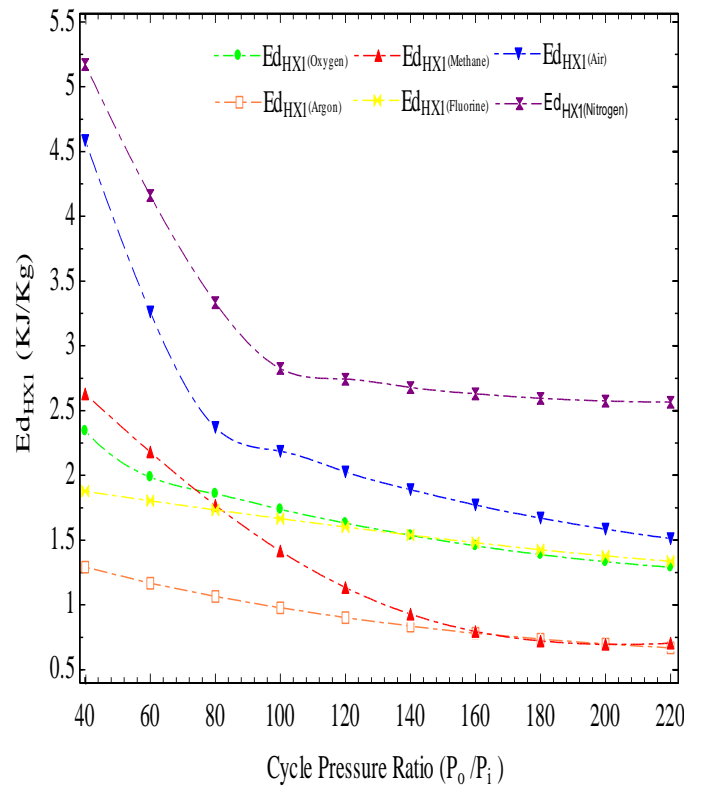


Figure 10: Variations in exergy destruction in HX1 with respect to cycle pressure ratio

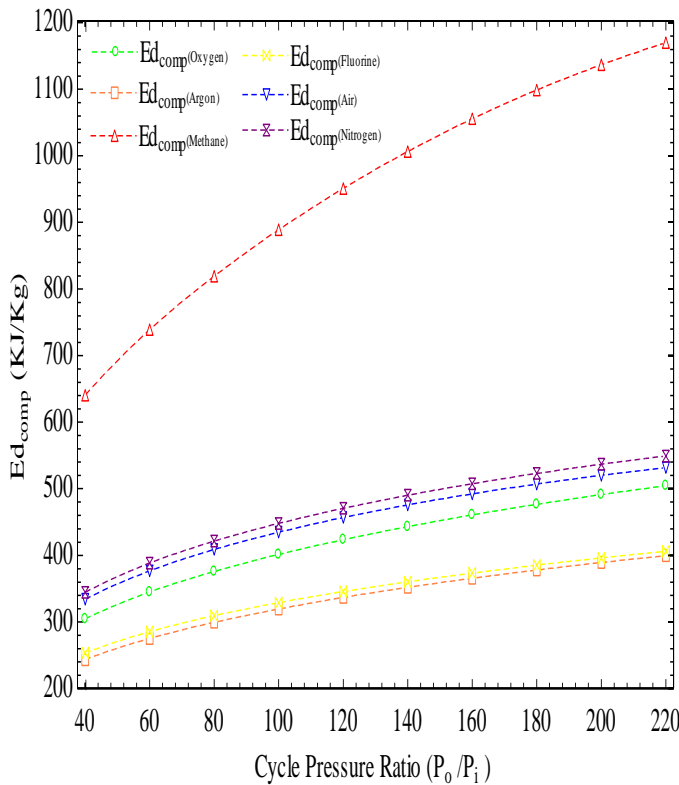


Figure 9: Variations in exergy destruction of compressor with cycle pressure ratio

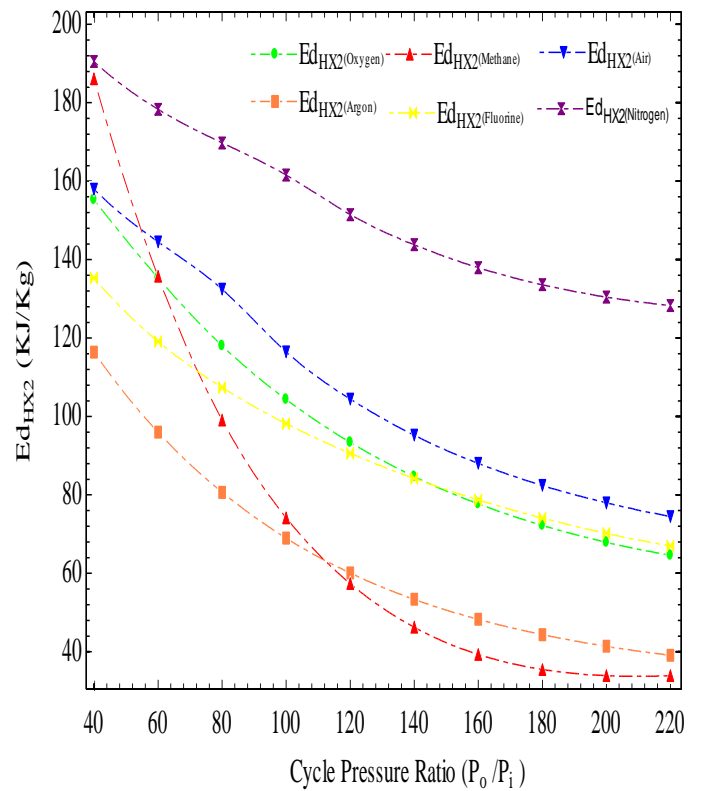


Figure 11: Variations in exergy destruction in HX2 with Cycle pressure ratio

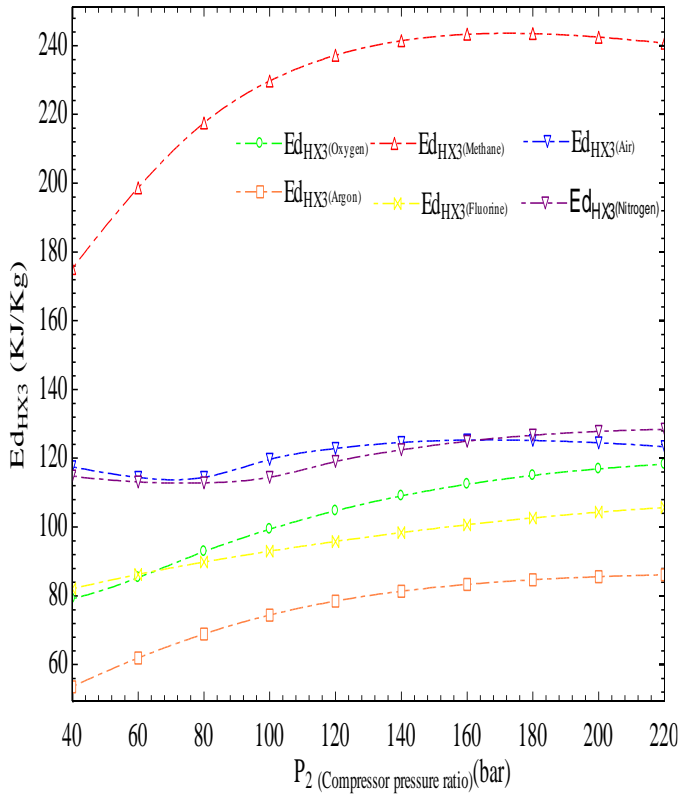


Figure 12: Variations in exergy destruction in HX3 with cycle pressure ratio

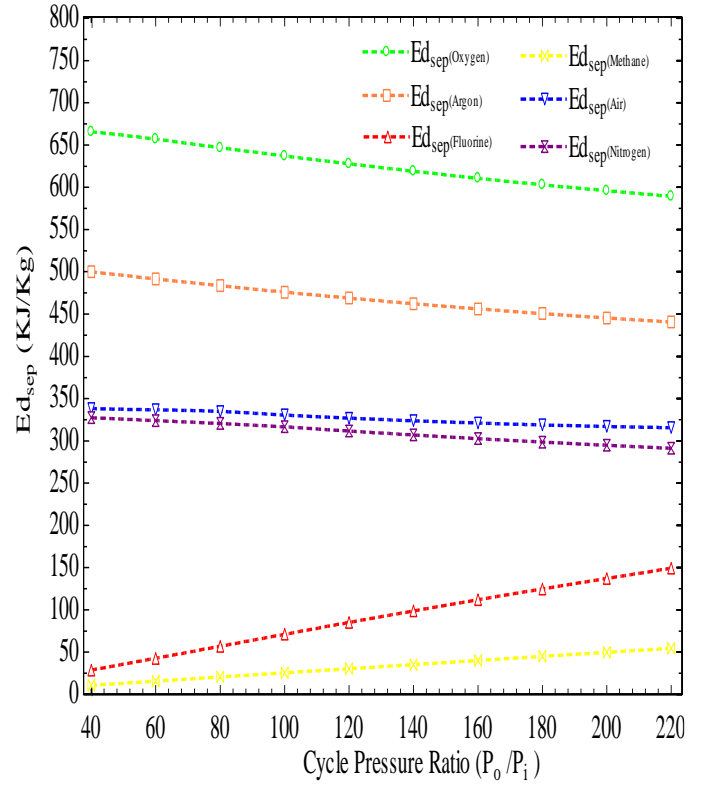


Figure 14: Variations in exergy destruction in separator with respect to cycle pressure ratio

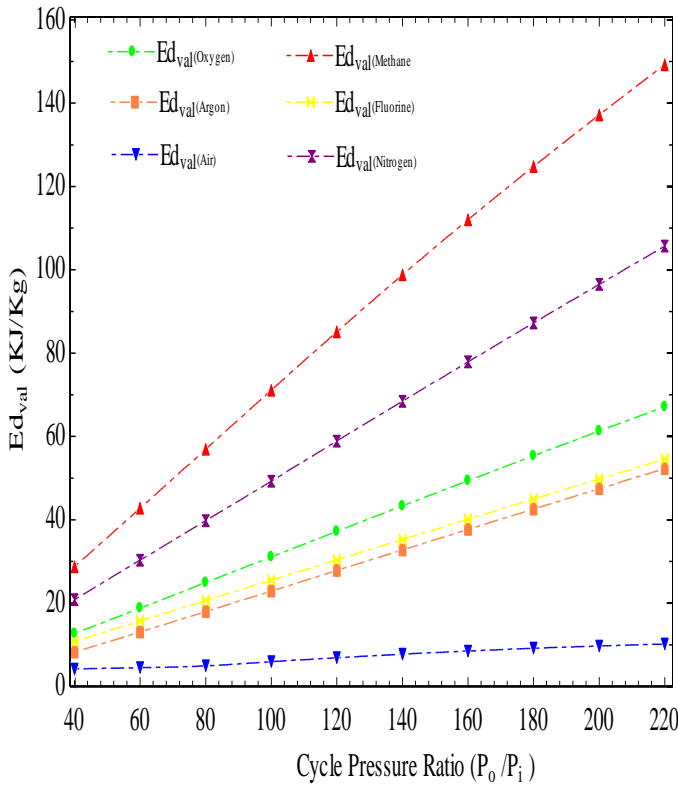


Figure 13: Variations in exergy destruction in valve with cycle pressure ratio

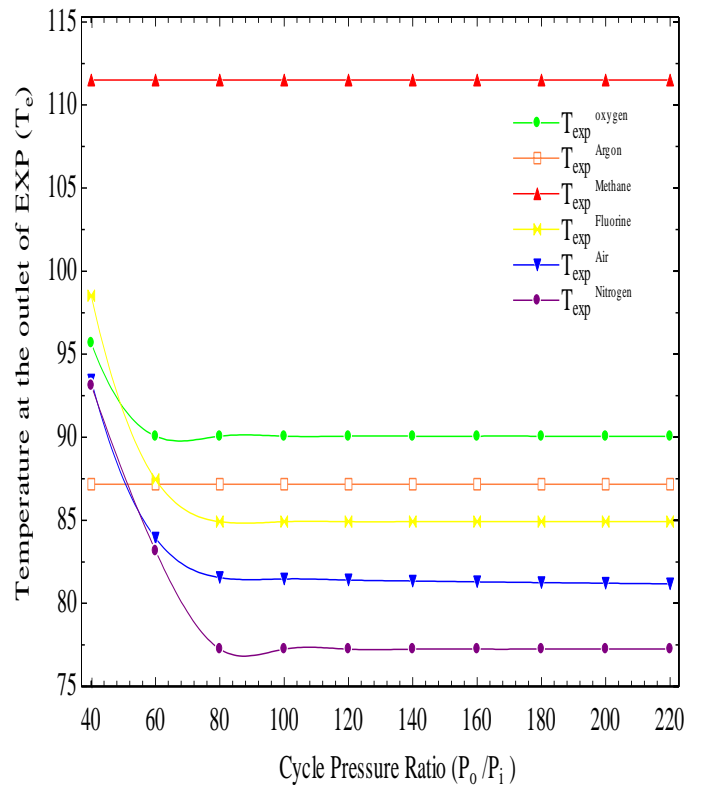


Figure 15: Variations in temperature at the outlet of expander with respect to cycle pressure ratio

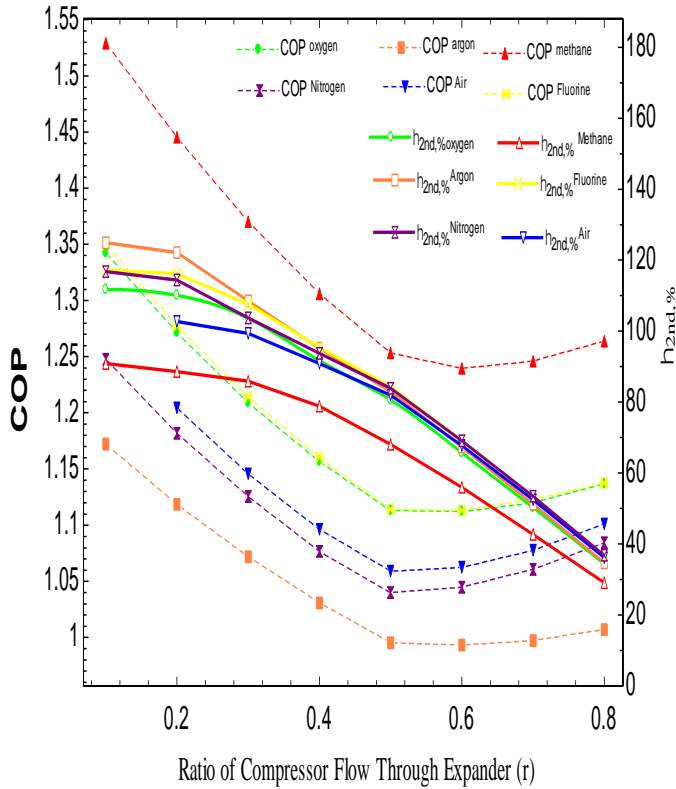


Figure 16: Variations in COP and second law efficiency with respect to ratio of compressor flow through expander

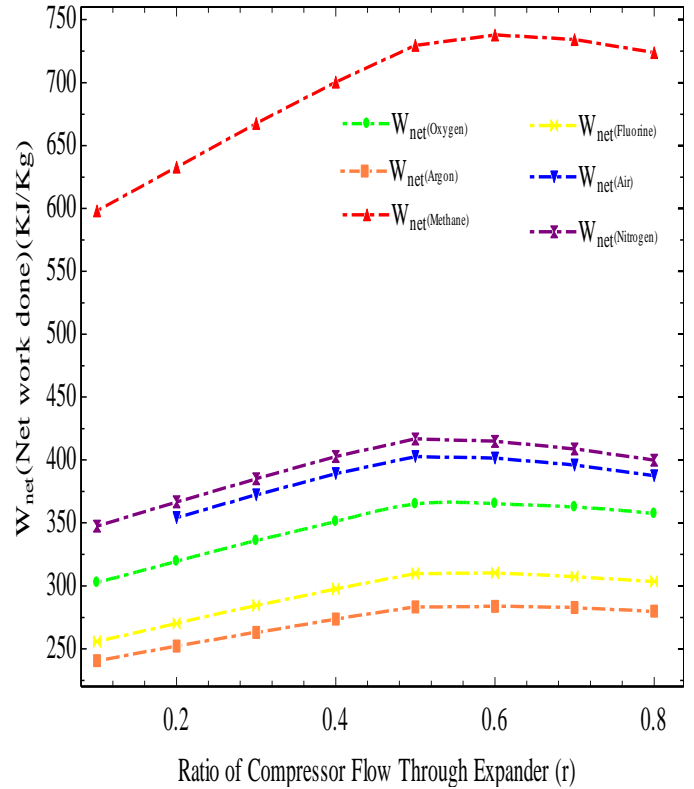


Figure 18: Variations in net work done with respect to the ratio of compressor flow through expander

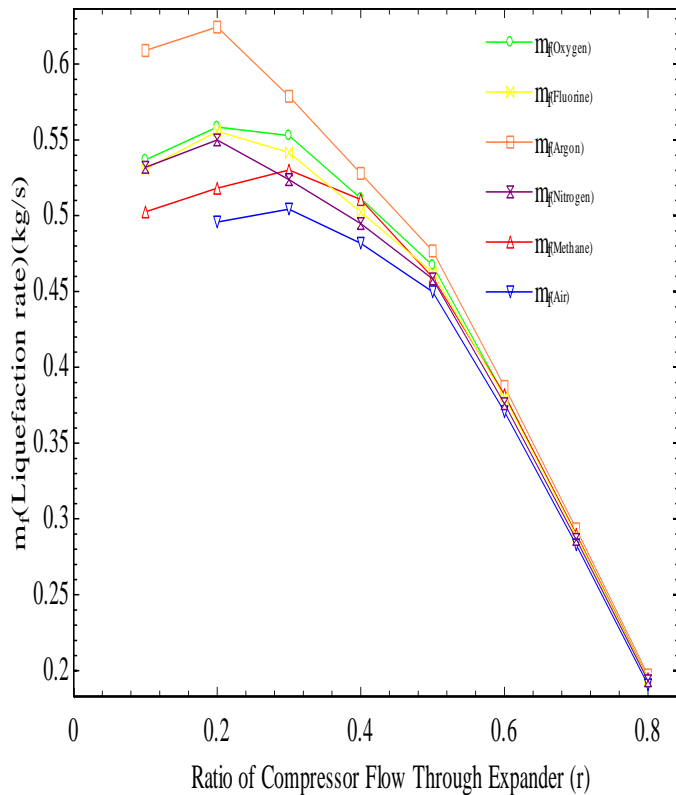


Figure 17: Variations in mass liquefaction rate with respect to ratio of compressor flow through expander

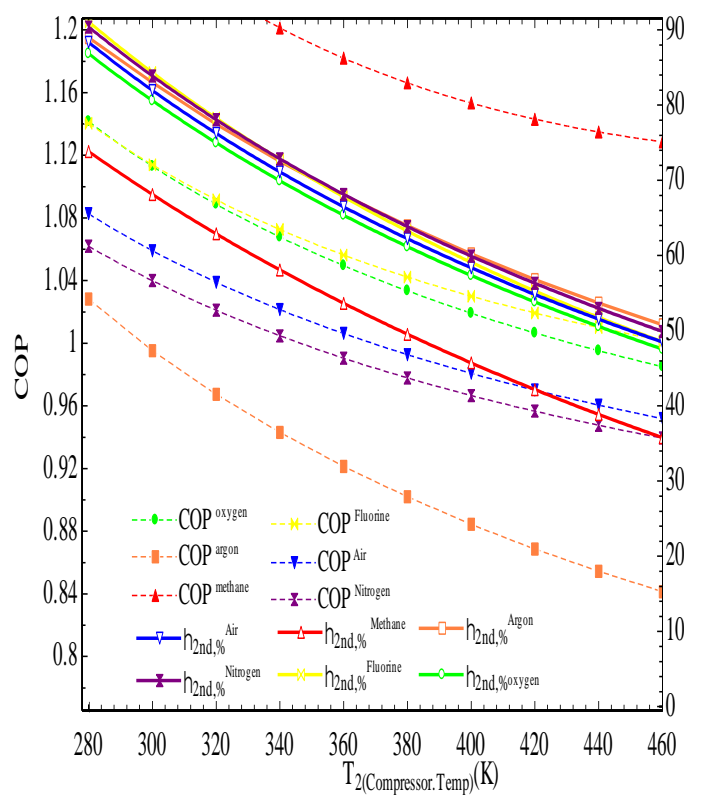


Figure 19: Variations in COP with respect to compressor temperature

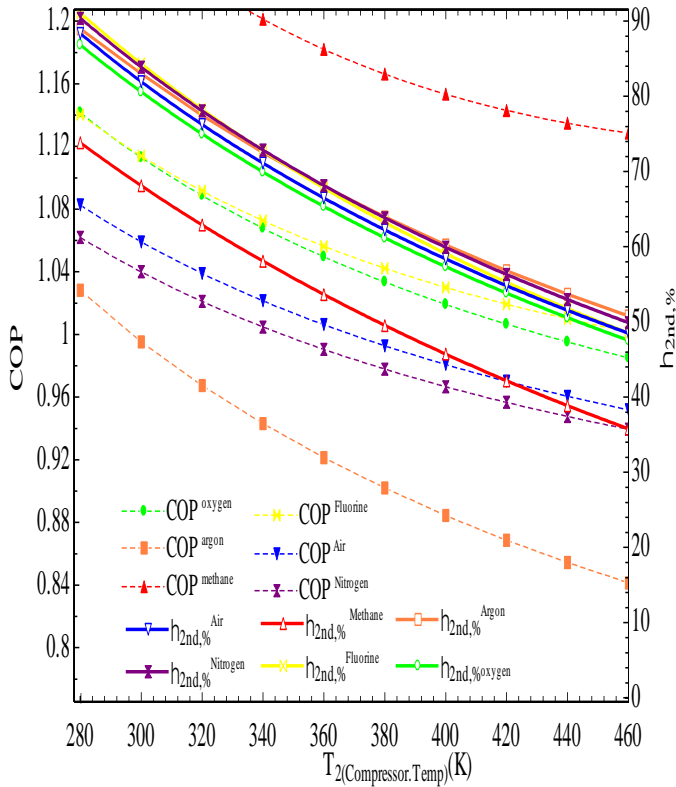


Figure 20: Variations in COP with respect to compressor temperature

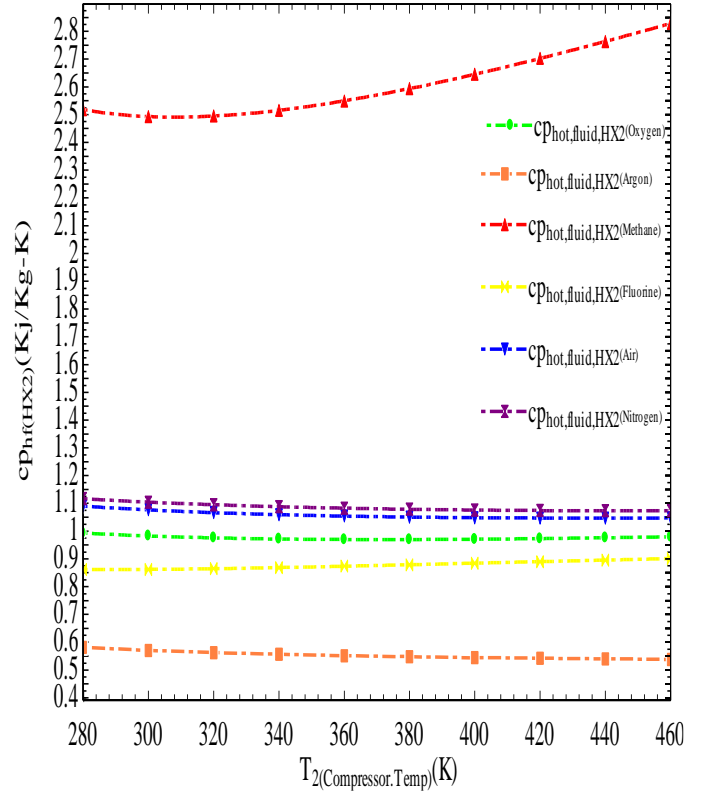


Figure 22: Variations in specific heat in HX2 with respect to compressor temperature

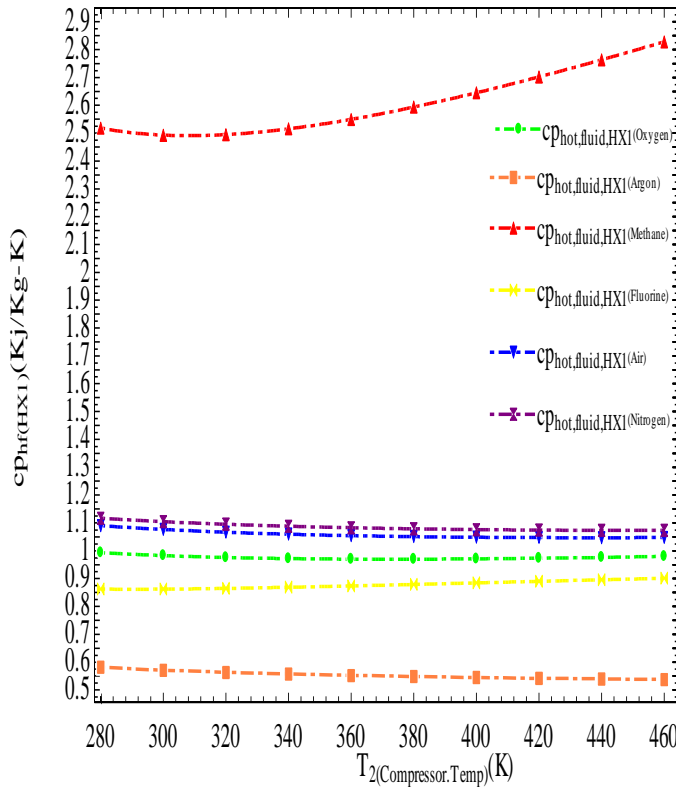


Figure 21: Variations in specific heat in HX1 with respect to compressor temperature

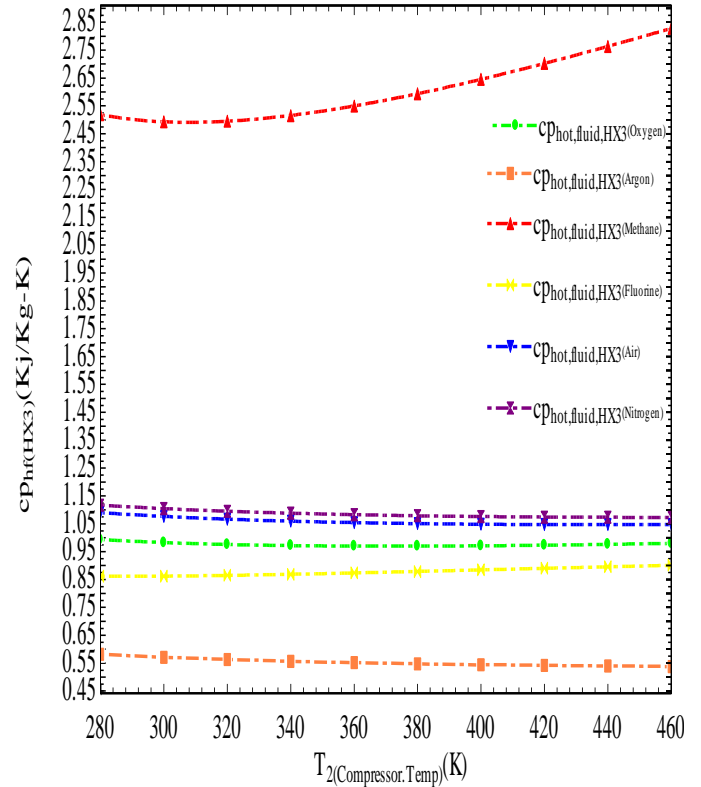


Figure 23: Variations in specific heat in HX3 with respect to compressor temperature

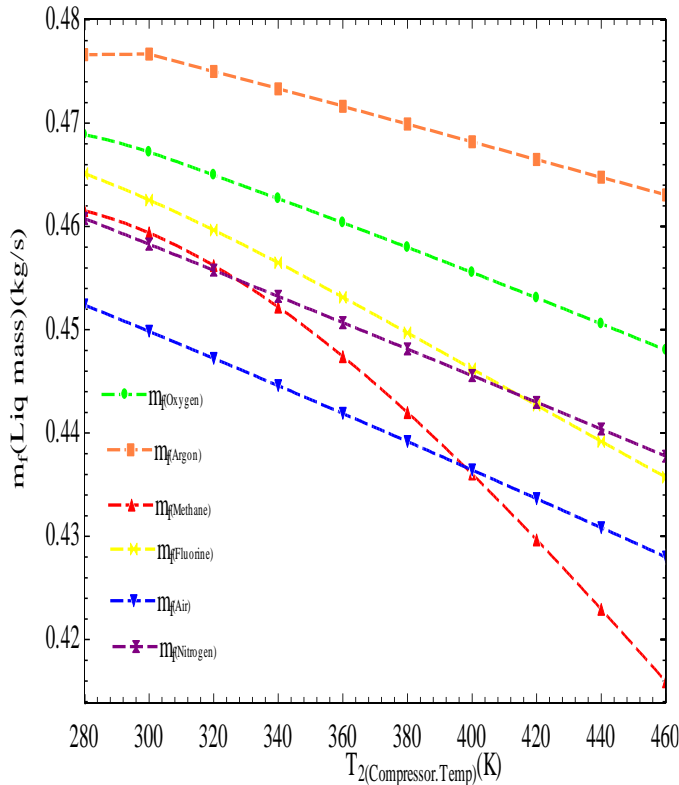


Figure 24: Variations in liquefaction mass flow rate with respect to compressor temperature

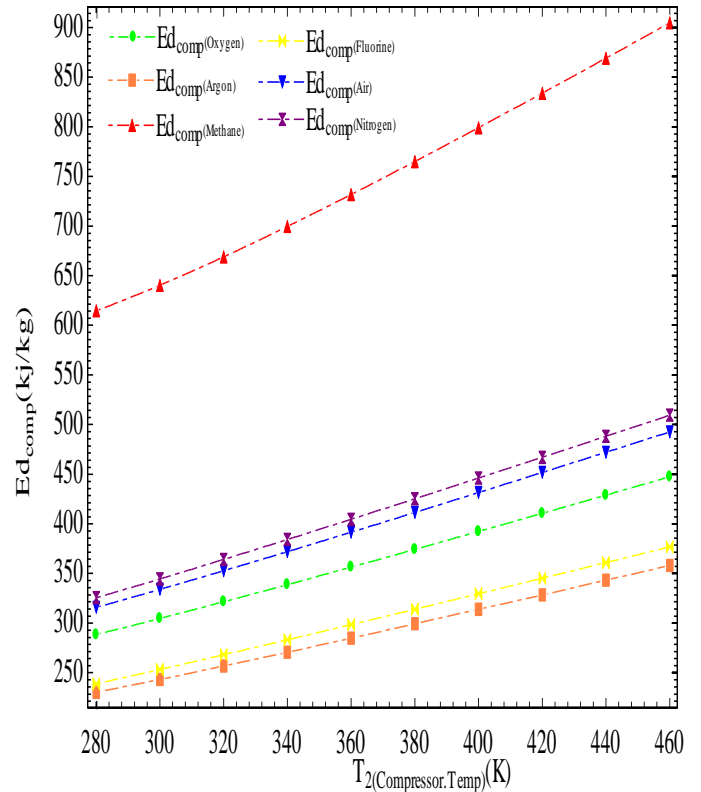


Figure 26: Variations in exergy destruction in Compressor with respect to compressor Temperature

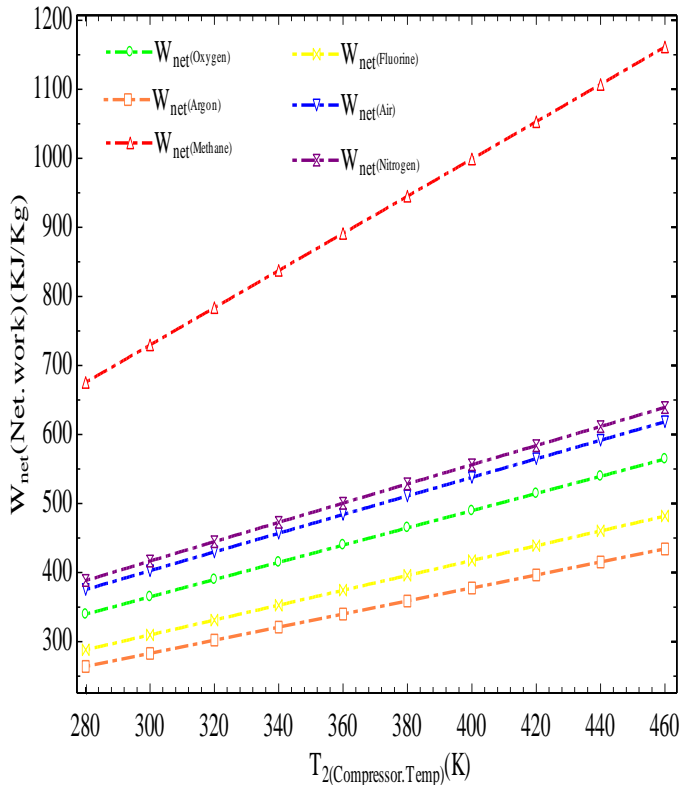


Figure 25: Variations in net work done with respect to compressor temperature

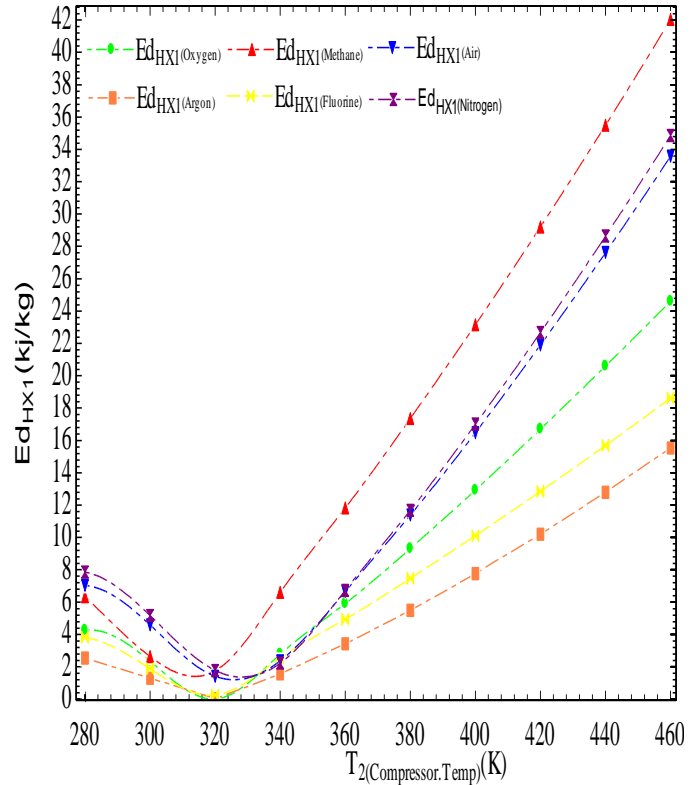


Figure 27: Variations in exergy destruction in HX1 with respect to compressor temperature

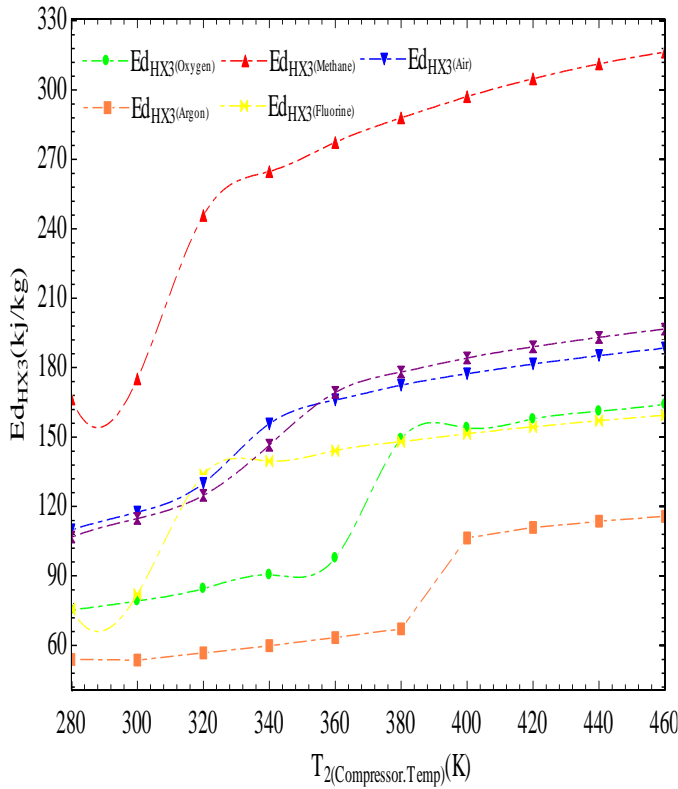


Figure 28: Variations in exergy destruction in HX2 with respect to compressor temperature

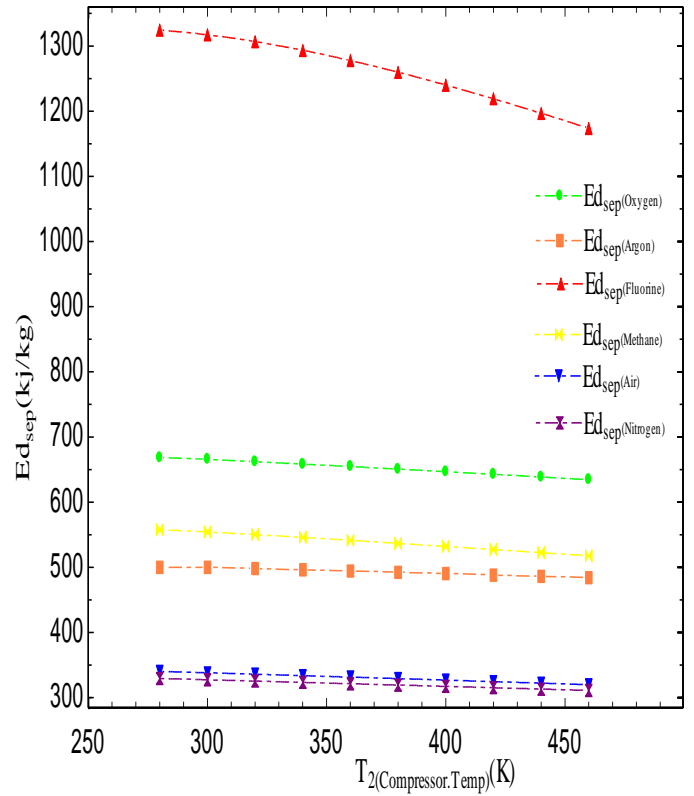


Figure 30: Variations in exergy destruction in compressor with compressor temperature

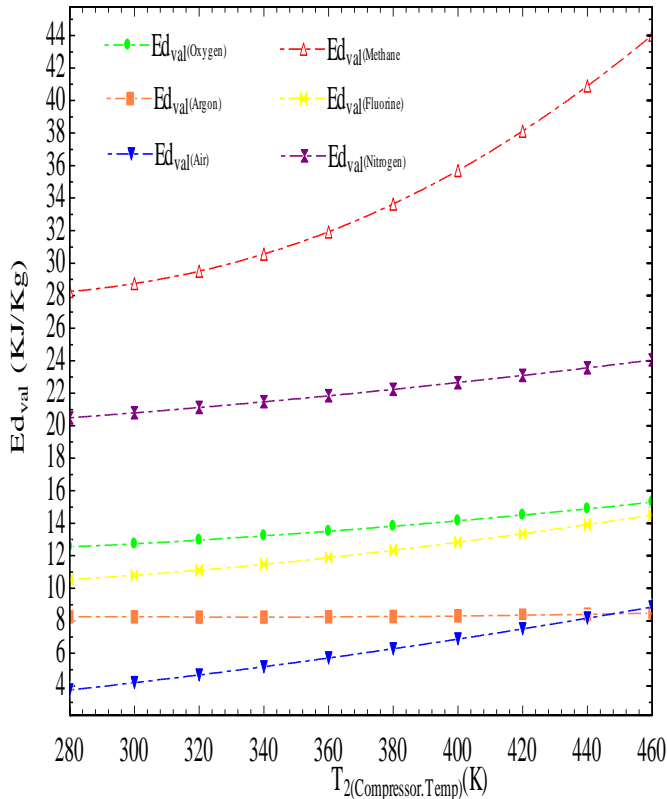


Figure 29: Variations in exergy destruction in HX3 with compressor temperature

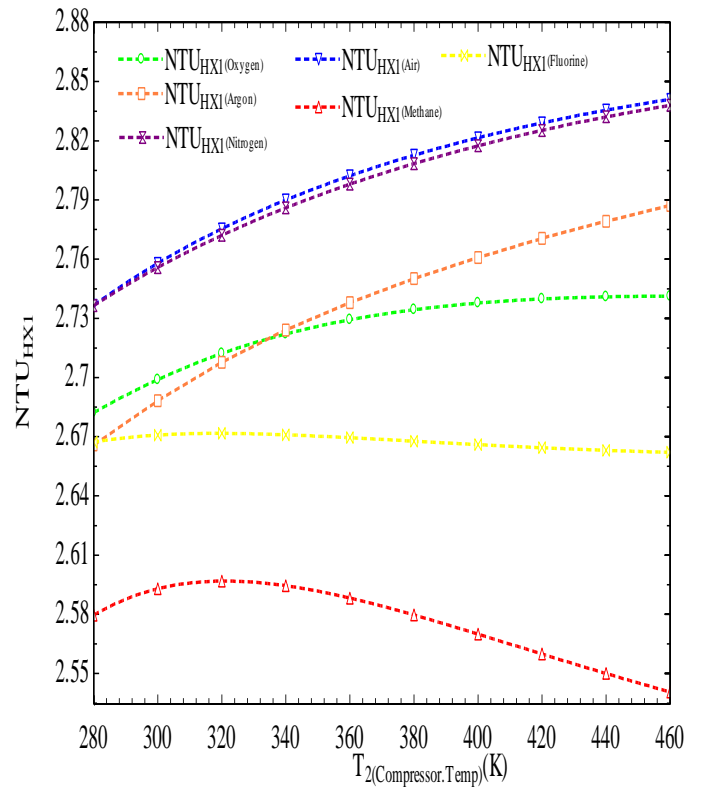


Figure 31: Variations in NTU in HX1 with compressor temperature

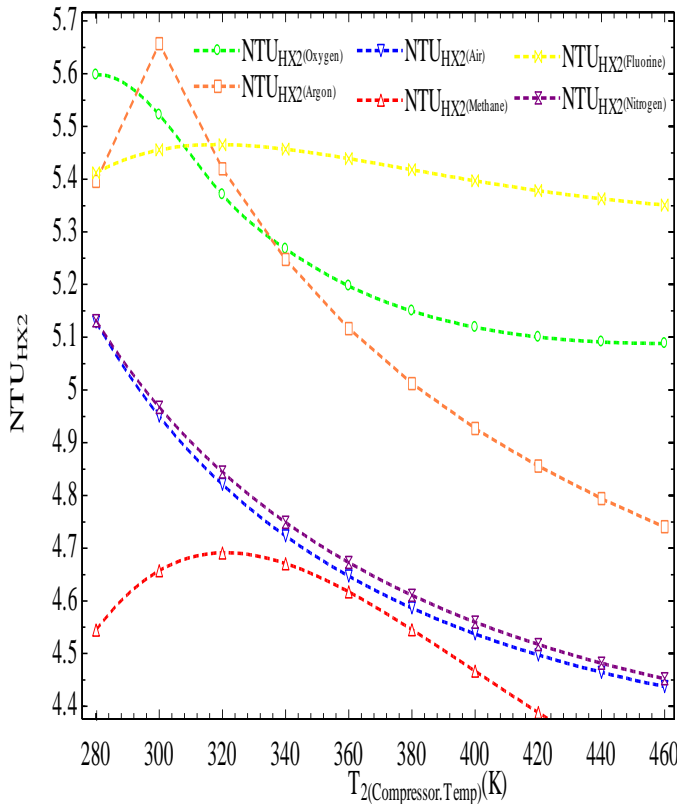


Figure 32: Variations in NTU in HX2 with compressor temperature

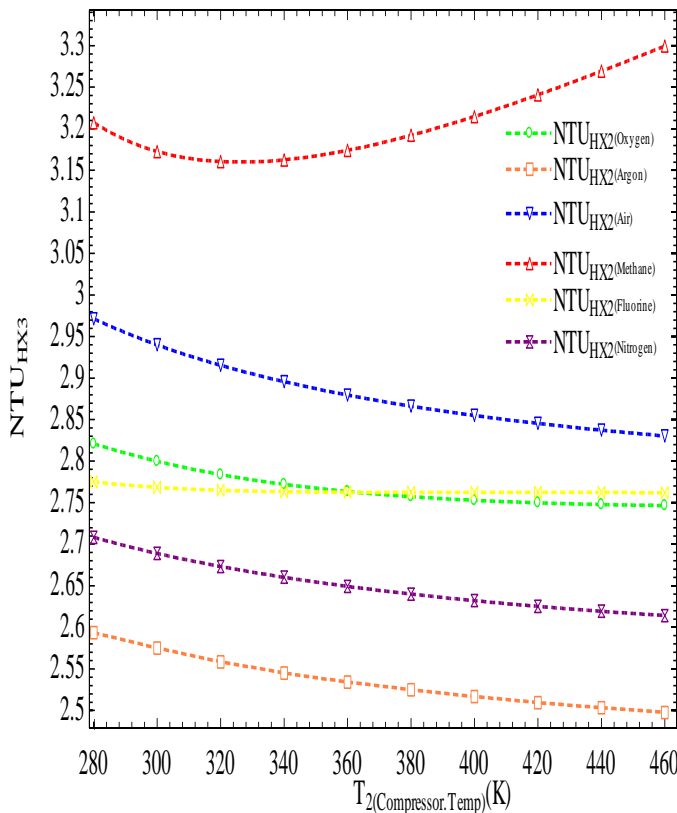


Figure 33: Variations in NTU in HX3 with compressor temperature

Figure 29 show exergy destruction rate in third heat exchanger with respect to compressor outlet temperature. In third heat exchanger the methane and fluorine gas show same trend of exergy destruction, both gas exergy destruction rate first decreases and then start increasing up to 460 K. Other remaining four gases shows increase in exergy destruction rate with increases in outlet compressor temperature. Exergy destruction rate in valve with respect to compressor outlet temperature is explained in fig.31. At 280 K, methane show 28 kJ/kg exergy destruction which increases up to 42 kJ/kg at 460 K. Gases like nitrogen show almost pressure range 280 K - 460 K. In fig.32, all gases exergy destruction rate in separator decreases with increase in compressor temperature. Fig.33 shows the variations in NTU in HX3 with compressor temperature.

3. Conclusions and Recommendations

- (1) COP and second law efficiency decrease with increase in pressure ratio. For Methane gas COP decreases.
- (2) Second law efficiency of system is highest for fluorine gas followed by nitrogen, air oxygen respectively which has 80-83% and methane gas shows lowest second law efficiency is which continuously decreases.
- (3) Gases such as argon, oxygen and methane show sharp decrease in liquefaction rate with increase in PR while gases fluorine, nitrogen and air show slight decrease as compared to above gases with increase in pressure ratio (PR). The liquefaction decrement rate of air is lowest.
- (4) The methane gas show highest requirement of work and argon required lowest. The trend of gases work requirement is progressing with increase in compressor temperature.
- (5) Specific heat for all gases increases during heat exchange with increases in pressure ratio (PR) of compressor. Methane gas show large change in specific heat 2 as compare to other gases with increase in PR. Other gases such as nitrogen, air, and oxygen of first heat exchanger (HX1) show very slight change in specific heat while the fluorine show lowest specific heat.
- (6) Methane gas show highest value of NTU among all gases and it varies with pressure ratio.
- (7) The exergy destruction rate in first heat exchanger is very low at low temperature. Most of the gases first show decreases in exergy destruction up to 320 K and then start increasing at very fast rate if compressor temperature is further increased. Methane gas show highest destruction rate.
- (8) In third heat exchanger the methane and fluorine gas show same trend of exergy destruction, both gas exergy destruction rate first decreases and then start increasing.
- (9) For all gases exergy destruction rate in separator decreases with increase in compressor temperature.
- (10) In second heat exchanger the variation in exergy destruction rate of methane and fluorine gas is first increases up to 300 K and then start decreasing on increasing compressor temperature. Gases such as

oxygen, air and argon are not much affected

References

- [1] Yu. V. Sinyavskii, Electrocaloric refrigerators: A promising alternative to current low-temperature Apparatus, *Chemical and Petroleum Engineering*, 31(6), 1995, 295-306
- [2] R. Agrawal, D. W. Woodward, Efficient cryogenic nitrogen generators: An exergy analysis, *Gas Separation & Purification*, 5(3), 1991, 139-150.